# MR imaging of the temporomandibular joint: Comparison between acquisitions at 7.0 Tesla using dielectric pads and 3.0 Tesla

Kuhn, Felix P ; Spinner, Georg ; Del Grande, Filippo ; Wyss, Michael ; Piccirelli, Marco ; Erni, Stefan ; Pfister, Pascal ; Ho, Michael ; Sah, Bert-Ram ; Filli, Lukas ; Ettlin, Dominik A ; Gallo, Luigi M ; Andreisek, Gustav ; Manoliu, Andrei

Abstract: OBJECTIVES To qualitatively and quantitatively compare MR imaging of the temporomandibular joint (TMJ) at 7.0 T using high-permittivity dielectric pads and 3.0 T using a clinical high-resolution protocol. METHODS IRB approved study with written informed consent. 12 asymptomatic volunteers were imaged at 7.0T and 3.0T using 32-channel head coils. High-permittivity dielectric pads consisting of barium titanate in deuterated suspension were used for imaging at 7.0T. Imaging protocol consisted of oblique sagittal PDw-TSE sequences. For quantitative analysis, pixel-wise signal-to-noise ratio (SNR) maps of the TMJ were calculated. For qualitative analysis, images were evaluated by two independent readers using 5-point Likert-scales. Quantitative and qualitative results were compared using t-tests and Wilcoxon signed-rank tests, respectively. RESULTS TMJ imaging at 7.0T using high-permittivity dielectric pads was feasible in all volunteers. Quantitative analysis showed similar SNR for both field strengths (mean±SD; 7.0T, 13.02±3.92; 3.0T, 14.02±3.41; two-sample t-tests, p = 0.188). At 7.0T, qualitative analysis yielded better visibility of all anatomical subregions of the temporomandibular disc (anterior band, intermediate zone, posterior band) compared to 3.0T (Wilcoxon signed-rank tests, $p<0.05$, corrected for multiple comparisons). CONCLUSIONS MR imaging of the TMJ at 7.0 T using high-permittivity dielectric pads yields superior visibility of the temporomandibular disc compared to 3.0T.

DOI: https://doi.org/10.1259/dmfr.20160280

# MR imaging of the temporomandibular joint: Comparison between acquisitions at 7.0 Tesla using dielectric pads and 3.0 Tesla

Running title: MR imaging of the temporomandibular joint at 7.0 T and 3.0 T

**Original Research**

Felix P. Kuhn, MD, MAS[1]

Georg Spinner, MSc[2]

Filippo Del Grande, MD[3]

Michael Wyss, BSc[2]

Marco Piccirelli, PhD[4]

Stefan Erni[5]

Pascal Pfister, MD[1]

Michael Ho, MD[1]

Bert-Ram Sah, MD[1]

Lukas Filli, MD[1]

Dominik A. Ettlin, MD, DMD[5]

Luigi M. Gallo, PhD[5]

Gustav Andreisek, MD, MBA[1]

Andrei Manoliu, MD, PhD[1,2,6]

[1] Institute for Diagnostic and Interventional Radiology, Department of Radiology, University Hospital Zurich, University of Zurich, Switzerland

[2] Institute for Biomedical Engineering, University of Zurich and ETH Zurich, Switzerland

[3]Department of Diagnostic and Interventional Radiology, Ospedale Regionale di Lugano, Switzerland

[4] Department of Neuroradiology, University Hospital Zurich, University of Zurich, Switzerland

[5]Center of Dental Medicine of the University of Zurich, Switzerland

[6]Psychiatric University Hospital, Department of Psychiatry, Psychotherapy and Psychosomatics, University of Zurich, Zurich, Switzerland

**Corresponding Author:**
Andrei Manoliu, MD, PhD,
Department of Radiology, University Hospital Zurich, Ramistrasse 100, 8091 Zurich, Switzerland
E-Mail: andrei.manoliu@usz.ch
Office: +41 44 255 2900
Current working address:
Department of Psychiatry, Psychotherapy and Psychosomatics, Psychiatric University Hospital Zurich, University of Zurich, Lenggstrasse 31, 8032 Zurich, Switzerland
Email: andrei.manoliu@puk.zh.ch
Office: +41 44 3842411

**Full contact details for each author:**

*Felix Kuhn, MD, MAS*
*Institute of Diagnostic Radiology, University Hospital Zurich, University of Zurich*
*Rämistrasse 100, 8091 Zurich, Switzerland*
*Phone: +41 44 255 29 00*
*Fax: +41 44 255 44 43*
*Email: felix.kuhn@usz.ch*

*Georg Spinner, MSc*
*Institute for Biomedical Engineering, University and ETH Zurich,*
*Gloriastrasse 35, 8092 Zurich, Switzerland*
*Phone: +41 44 632 53 25*
*Fax: +41 44 632 11 93*
*Email: spinner@biomed.ee.ethz.ch*

*Fillipo Del Grande, MD, MBA*
*Department of Diagnostic and Interventional Radiology, Ospedale Regionale di Lugano*
*Via Tesserete. 6900, Lugano, Switzerland*
*Phone: +41 91 811 6091*
*Email: fdelgra1@jhmi.edu*

*Michael Wyss, BSc*
*Institute for Biomedical Engineering, University and ETH Zurich*
*Gloriastrasse 35, 8092 Zurich, Switzerland*
*Phone: +41 44 255 30 53*
*Fax: +41 44 632 11 93*
*Email: wyss@biomed.ee.ethz.ch*

*Marco Piccirelli, PhD*
*Department of Neuroradiology, University Hospital Zurich and University of Zurich*
*Frauenklinikstrasse 10, 8091 Zurich, Switzerland*
*Phone: +41 44 255 56 00*
*Fax: +41 44 255 45 04*
*Email: Marco.Piccirelli@usz.ch*

*Stefan Erni*
*Center of Dental Medicine of the University of Zurich*
*Plattenstrasse 11, 8032 Zurich, Switzerland*
*Phone: +41 44 634 3311*
*Fax: +41 44 634 4311*
*Email: Stefan.Erni@zzm.uzh.ch*

*Pascal Pfister, MD*
*Institute of Diagnostic Radiology, University Hospital Zurich, University of Zurich,*
*Rämistrasse 100, 8091 Zurich, Switzerland*
*Phone: +41 44 255 29 00*
*Fax: +41 44 255 44 43*
*Email: pascalpfister89@hotmail.com*

*Michael J. Ho, MD*
*Institute of Diagnostic Radiology, University Hospital Zurich, University of Zurich,*
*Rämistrasse 100, 8091 Zurich, Switzerland*
*Phone: +41 44 255 29 00*
*Fax: +41 44 255 44 43*
*Email: Michael.Ho@usz.ch*

*Bert-Ram Sah, MD*
*Institute of Diagnostic Radiology, University Hospital Zurich, University of Zurich*
*Rämistrasse 100, 8091 Zurich, Switzerland*
*Phone: +41 44 255 29 00*
*Fax: +41 44 255 44 43*
*Email: bert-ram.sah@usz.ch*

*Lukas Filli, MD*
*Institute of Diagnostic Radiology, University Hospital Zurich, University of Zurich,*
*Rämistrasse 100, 8091 Zurich, Switzerland*
*Phone: +41 44 255 29 00*
*Fax: +41 44 255 44 43*
*Email: Lukas.Filli@usz.ch*

*Dominik. A. Ettlin, MD, DMD*
*Center of Dental Medicine of the University of Zurich*
*Plattenstrasse 11, 8032 Zurich, Switzerland*
*Phone: +41 44 634 3311*
*Fax: +41 44 634 4311*
*Email: Dominik.Ettlin@zzm.uzh.ch*

*Luigi M. Gallo, PhD*
*Center of Dental Medicine of the University of Zurich*
*Plattenstrasse 11, 8032 Zurich, Switzerland*
*Phone: +41 44 634 3311*
*Fax: +41 44 634 4311*
*Email: Luigi.Gallo@zzm.uzh.ch*

*Gustav Andreisek, MD, MBA*
*Institute of Diagnostic Radiology, University Hospital Zurich, University of Zurich*
*Rämistrasse 100, 8091 Zurich, Switzerland*
*Phone: +41 44 255 49 22*
*Fax: +41 44 255 44 43*
*Email: gustav@andreisek.de*

*Andrei Manoliu, MD, PhD*
*Institute of Diagnostic Radiology, University Hospital Zurich, University of Zurich,*
*Rämistrasse 100, 8091 Zurich, Switzerland*
*Phone: +41 44 255 29 00*
*Fax: +41 44 255 44 43*
*Email: andrei.manoliu@usz.ch*

*Current working address:*
*Department of Psychiatry, Psychotherapy and Psychosomatics, Psychiatric University Hospital Zurich, University of Zurich, Lenggstrasse 31, 8032 Zurich, Switzerland*
*Phone: +41 44 3842411*
*Fax: +41 44 3834456*
*Email: andrei.manoliu@puk.zh.ch*

**Acknowledgements / Grant support information:**

The local IRB approved the current prospective MR imaging study in asymptomatic volunteers. Written informed consent was obtained from all participants. The study was registered in the official research data base of the University of Zurich, Switzerland. This study was funded by the Swiss National Science Foundation (#320030_156466/1).

**Abstract**

Objectives:

To qualitatively and quantitatively compare MR imaging of the temporomandibular joint (TMJ) at 7.0 T using high-permittivity dielectric pads and 3.0 T using a clinical high-resolution protocol.

Methods:

IRB approved study with written informed consent. 12 asymptomatic volunteers were imaged at 7.0T and 3.0T using 32-channel head coils. High-permittivity dielectric pads consisting of barium titanate in deuterated suspension were used for imaging at 7.0T. Imaging protocol consisted of oblique sagittal PDw-TSE sequences. For quantitative analysis, pixel-wise signal-to-noise ratio (SNR) maps of the TMJ were calculated. For qualitative analysis, images were evaluated by two independent readers using 5-point Likert-scales. Quantitative and qualitative results were compared using t-tests and Wilcoxon signed-rank tests, respectively.

Results:

TMJ imaging at 7.0T using high-permittivity dielectric pads was feasible in all volunteers. Quantitative analysis showed similar SNR for both field strengths (mean±SD; 7.0T, 13.02±3.92; 3.0T, 14.02±3.41; two-sample t-tests, $p = 0.188$). At 7.0T, qualitative analysis yielded better visibility of all anatomical subregions of the temporomandibular disc (anterior band, intermediate zone, posterior band) compared to 3.0T (Wilcoxon signed-rank tests, $p<0.05$, corrected for multiple comparisons).

Conclusions:

MR imaging of the TMJ at 7.0 T using high-permittivity dielectric pads yields superior visibility of the temporomandibular disc compared to 3.0T.

Keywords:

Magnetic resonance imaging; Temporomandibular Joint; Temporomandibular Joint Disc; Magnetic Fields; Signal-To-Noise Ratio

## Introduction

Over the last decades, magnetic resonance imaging (MRI) of the temporomandibular joint (TMJ) has emerged as state of the art to assess pathologies underlying temporomandibular disorders (TMDs),[1,2] such as structural alterations or displacement of the temporomandibular disc.[3, 4] Currently MR imaging of the TMJ is performed mainly at 1.5 Tesla (T) or 3.0 T.[5, 6] However, MRI results are still falling short of showing a clear association with reported symptoms.[7] Furthermore, the impact of potential imaging findings on treatment choice and clinical outcome is still controversial,[7] suggesting that the depiction of the TMJ in clinical routine is still unsatisfactory and may benefit from further optimization.

One explanation for the mismatch between clinical presentation of patients suffering from TMDs and MR imaging findings might be the insufficient performance of current standard MRI hardware and/or imaging protocols to depict the clinically relevant, relatively small anatomical key structures of the TMJ, such as the different regions of the articular disc, in full detail. According to this theory, this would mean that the image resolution needs to be improved; however, at a preserved signal-to-noise ratio (SNR). To achieve this, optimized coil designs or higher static magnetic field strengths, such as 7.0 T could be used.[8, 9,10, 11] Since the obtainable SNR is intrinsically linked to the static magnetic field strength in a linear way, imaging the TMJ at 7.0 T should theoretically enable - compared to e.g. 3.0 T - a higher overall SNR where a portion of the signal increase might be inter alia utilized to enhance the spatial resolution.[12, 13]

Given those theoretical considerations, a growing number of studies are investigating

potential benefits of MR imaging the musculoskeletal system and/or head and neck regions at 7.0 T compared to 3.0 T, which is considered as standard reference in most cases.[14] Most of those studies reported superior performance of MR imaging at 7.0 T for the the knee, the wrist or the inner ear.[13-16] However, no study so far has assessed, whether MR imaging of the TMJ at 7.0 T might indeed yield superior performance compared to 3.0 Tesla when using optimized clinical sequences. The lack of studies in this area can be mainly explained by the fact that imaging the TMJ at 7.0 T is very challenging and limited by several TMJ-specific as well as general methodological reasons. First, specific receiver arrays for imaging the TMJ at 7 Tesla are still not commercially available, which is of particular importance for comparison studies since the coil design has a crucial influence on the SNR and makes it necessary to use standard head coils. Second, strong local inhomogeneities in the transmit radiofrequency field (B1+) caused by the elliptical head shape and susceptibility difference between different tissue types are considerably limiting the SNR in the lateral areas of the head, also affecting the areas where the TMJs are located. [15, 17, 18] In addition to those observations, several other general considerations are further complicating the realization of such studies. The intrinsic T1 time of soft tissue increases with higher field strength, which typically has to be addressed by longer repetition times and subsequently longer acquisition times, increasing the risk of movement artifacts.[19] In addition, different tissue relaxation properties might result in different effects of the higher magnetic field strength on SNR. [13] Furthermore, regarding SNR calculation, most of the commonly used algorithms do not account for the distinct spatial variations of noise levels, which are inter alia introduced by multi-channel imaging and provide therefore unreliable results, especially when comparing coils with a different number of receive channels.[13]

Recently, the feasibility of imaging the TMJ at 7.0T has been demonstrated for the first time using a commercially available 32-channel head coil and special high-permittivity dielectric pads consisting of barium titanate.[20] The pads increased the local B1+ fields in the areas covering the TMJs,[15] thus increasing the local SNR and facilitating imaging of the TMJ at 7.0T. Furthermore, aforementioned study provided first proof that intricate algorithms calculating SNR on a voxel-wise basis and taking noise correlation among channels into account was applicable for imaging the TMJ and yielded robust results.[13, 20] Nevertheless, a systematic evaluation of this novel approach to image the TMJ at 7.0 T with respect to the current benchmark exam, which is high-resolution MR imaging at 3.0 T, was not performed.

Therefore, the aim of the current study was to quantitatively and qualitatively compare MR imaging of the TMJ at 7.0 T utilizing high-permittivity dielectric pads with high-resolution 3.0 T imaging.

## Methods and materials

The local Institutional Review Board (IRB) approved the current prospective MR imaging study in asymptomatic volunteers. The IRB approval did not allow inclusion of patients. Thus, only asymptomatic volunteers could be included. Written informed consent was obtained from all participants. The study was registered in the official research data base of the University of (blinded).

*Study Subjects*

Twelve healthy asymptomatic volunteers were included in the current study (6 women, mean age 25.7 years, range, 20 – 29 years and 6 men, mean age 26.5 years, range 24 – 32 years). Inclusion criteria were willingness to participate in this study. Exclusion criteria were current or past symptoms related to TMD, pregnancy, claustrophobia and metallic implants.

*MR imaging*

*MR protocol*

MR imaging was performed on a 3.0T Philips Ingenia system (Philips Healthcare, Best, The Netherlands) using a 32-channel head coil (SENSE Head coil 32 elements, Philips Healthcare) and on a 7.0 T Philips Achieva system (Philips Healthcare, Cleveland, OH, USA) using a quadrature transmit head coil in combination with a 32-channel receive array (NOVA Medical, Wilmington, USA) and special high-permittivity dielectric pads (see bellow). Proton density weighted turbo spin echo (PDw-TSE) sequences in oblique sagittal planes were acquired using the sequence parameters presented in Table 1. To ensure a

correct angle, the planes were carefully oriented perpendicular to the transverse axis of the mandibular condyles according to recent studies performing clinical MR imaging of the TMJ [21, 22].

*Dielectric Pads*

For imaging the TMJ at 7.0 T, dielectric pads explicitly designed to improve the local B1+ field in the lateral areas of the head were used as described in a previous study.[20] Briefly, pads were manufactured using a suspension of barium titanate (325 mesh powder, Alfa Aesar GmbH & Co KG, Karlsruhe, Germany) and deuterated water (99.9%, Sigma Aldrich, Zwijndrecht, The Netherlands). The geometry of the manufactured pads was based on simulations performed by Brink and colleagues,[15] and resulted in two different sets of dielectric pads for female and male volunteers due to gender-specific difference in head size and B1+ dropouts (set for females: left side, 100 x 100 x 10 mm3; right side, 140 x 140 x 10 mm3; set for males: left side, 100 x 100 x 10 mm3; right side, 180 x 140 x 10 mm3, see Figure 1).

*Noise scans*

For all volunteers, an identical scan without RF excitation and gradient switching was performed subsequently to the aforementioned sequence at 7.0 T with dielectric pads and at 3.0 T without pads to measure the noise and enable a voxel-wise calculation of the SNR.

*Volunteer imaging*

All volunteers were scanned at 7.0 T using dielectric pads and at 3.0 T without dielectric pads. To avoid potential influence of the scan order on imaging results, volunteers were randomly assigned to the different magnetic field strengths with, in addition, half of the

volunteers even scanned at different days (mean time between the scans 1.1 ± 1.22 days). For MR imaging at 7.0 T, the dielectric pads were placed centered on both TMJs of each subject. All images were taken with the mouth closed.

*Data analysis*

*SNR measurements*

Analysis of measured SNR followed the procedure previously described in full detail.[20] Briefly, SNR was evaluated on a voxel-wise basis by post-processing the image data and corresponding measured noise for every coil channel using dedicated software routines (Matlab, Natick USA), which resulted in voxel-based SNR maps. According to Nordmeyer-Massner and colleagues and following a recently reported analysis algorithm,[13,20-22] SNR was calculated as follows:

$$SNR = \frac{|\rho|}{\sigma}$$

($\rho$, maximal magnitude of the transverse magnetization within a voxel;[23] $\sigma$, standard deviation of the corresponding noise components.[24] Subsequently, each TMJ disc, fossa and condyle were manually segmented for each SNR map. Corresponding SNR values were extracted, resulting in one SNR-value per tissue for each subject´s TMJ. Calculation of theoretical SNR for TSE sequences was performed as follows:

$$SNR \propto \frac{B_0\, VoxelSize}{\sqrt{BW}}\, pd\, e^{-\frac{TE}{T2}} \left(1 - e^{-\frac{TR}{T1}}\right) \sin\theta$$

where scanner parameters (flip angle (θ), static magnetic field ($B_0$)), tissue parameters (T1, T2, pd), and sequence parameters (voxel size, receiver bandwidth (BW)) are accounted for. The tissue parameters differences were taken into account by adapting the TE and TR. The flip angle was optimized using the dielectric pads. For the remaining parameters, the clinically meaningful constrain of similar water-fat shift at the two field strengths was

chosen. This implies a linear increase of the BW relative to the static magnetic field as described by following formula:

$$SNR \propto \frac{B_0\, VoxelSize}{\sqrt{BW}} \propto \sqrt{B_0}\, VoxelSize$$

*Qualitative image evaluation*

All images were anonymized (subject's initials blinded) and saved in the hospitals picture archiving and communication (PACS) system (Impax 6.0, Agfa Healthcare, Mortsel, Belgium). Subsequently, two fellowship-trained radiologists assessed independently all images (initials blinded) with respect to the overall image quality as well as to the visibility of following clinically relevant structures: (i) articular disc (anterior band, intermediate zone, posterior band), (ii) bilaminar zone, (iii) mandibular fossa, (iv) mandibular condyle and (v) inferior lateral pterygoid muscle. The radiologists were blinded to the volunteers` details, field strength and the fact whether the 7.0 T or the 3.0 T images were performed first. Images were shown to them randomly. The visibility of aforementioned anatomical structures was graded on a 5-point Likert-Scale (1, excellent visibility and delineation; 5, complete lack of visibility). [5]

*Statistical Analysis*

All statistical analyses were performed using SPSS (release 22.0, SPSS Inc., Chicago, IL). Shapiro-Wilk tests were performed to test for normal distribution of the SNR. Paired-sample t-tests were performed to assess differences between images acquired at 7.0 T and 3.0 T (significance level $\alpha$=0.05) regarding SNR. Two-sample t-tests were used to evaluate potential differences in SNR between male and female volunteers at 7.0 T and 3.0 T (significance level $\alpha$=0.05). To evaluate statistically significant differences between the images acquired at 7.0 T and 3.0 T with respect to the visibility of the anatomical

structures of the TMJ as well as the overall image quality, Wilcoxon signed-rank tests were performed (significance level $\alpha$=0.05, corrected for multiple comparisons (n=8 according to the number of assessed anatomical structures)). To evaluate potential differences between gender groups regarding the visibility of the TMJ´s structures, Mann-Whitney-U tests were performed (significance level $\alpha$=0.05, corrected for multiple comparisons (n=8 according to the number of assessed anatomical structures)). To assess the inter-reader agreement in the qualitative MR image analysis, Kappa-statistics was used. Kappa values of 0.41 – 0.60 were considered as moderate agreement, values of 0.61 – 0.80 were considered as substantial agreement, values of 0.81 – 0.99 were considered as almost perfect agreement and values of 1.00 were considered as perfect agreement.[25]

## Results

All images were successfully acquired. Specific absorption rate (SAR) remained below individual limits in all sequences. No volunteer reported side effects during the scan.

*Quantitative analysis*

SNR analysis within the areas of interest (temporomandibular disc, the temporomandibular fossa and the temporomandibular condyle) yielded normal distribution for both field strengths (7.0 T, p=0.486; 3.0 T, p=0.359). The absolute SNR values were not different for both field strengths (mean±SD; 7.0 T, 13.02±3.92; 3.0 T, 14.02±3.41; p = 0.19, see Figure 2). There was no gender-specific difference in SNR at 7.0 T using dielectric pads (mean±SD; women, 13.18±4.31; men, 12.86±3.68; p = 0.85) and at 3.0 T (mean±SD; women, 14.23±4.17; men, 13.82±;2.60 p = 0.78). According to the formula described in the methods section and taking all sequence parameters into account, the the theoretical SNR difference between 3.0 T and 7.0 T is:

$$\frac{SNR_{7T}}{SNR_{3T}} = \sqrt{\frac{7}{3}}\,\frac{16}{25} = 0.98$$

This demonstrates that the whole SNR increase due to the higher B0 has been invested in increased resolution together with similar water-fat shift.

*Qualitative analysis*

Twenty-four images of the TMJs of 12 subjects were compared between 7.0 T and 3.0 T with respect to the visibility of the anatomical structures of the TMJ (Table 2). Inter-reader agreement ranged from “substantial” to “almost perfect” for 7.0 T (0.63 – 0.84) and 3.0 T (0.76 – 0.87). For both readers, imaging the TMJ at 7.0 T yielded significantly increased

visibility of all small anatomical structures, i.e. of the different zones of the temporomandibular disc, including the anterior band, the intermediate zone and the posterior band ($p<0.05$, corrected for multiple comparisons , see Table 2). It is to note that the visibility of the larger anatomical structures, namely the bilaminar zone, the mandibular fossa, the mandibular condyle and the inferior pterygoid muscle was similar for both field strengths. Overall image quality was not different when compared between 7.0 T and 3.0 T ($p<0.05$, corrected for multiple comparisons, see Figure 3 and Table 2). There was no statistically significant difference in the visibility of anatomical structures between female and male volunteers (Table 3, $p<0.05$, corrected for multiple comparisons).

## Discussion

In the current study, we found that imaging the TMJ at 7.0 T provides better visibility of small anatomical structures compared to standard-of-care 3.0T MR imaging. This was mainly yielded by a higher spatial resolution while overall SNR could be kept similar. Therefore, the current results suggest that imaging the TMJ at 7.0 T using high-permittivity dielectric pads might be feasible in the clinical routine and the diagnosis of disc pathologies could be improved through a better visibility of the underlying anatomy.

*High-permittivity dielectric pads*

Until now, imaging the TMJ at 7.0 T was not performed due to considerable challenges, one of which are strong local transmit radiofrequency field (RF; B1+) inhomogeneities, causing an inhomogeneous flip-angle distribution within the head, particularly with higher flip angles at the center and lower flip angles at the lateral regions, overlapping with the areas covering the TMJ.[18] Recently, Manoliu et al solved this problem by using specifically tailored high-permittivity dielectric pads consisting of barium titanate in deuteraded water,[20] which can be used to mitigate the B1+ dropouts within the temporal bone at cost of the global B1+ field.[15, 17, 26] In the current study, identical high-permittivity dielectric pads were used to enable imaging the TMJ at 7.0 T. Our pads were differently designed for female and male volunteers to take gender-specific differences in head size into account. However, qualitative and quantitative analysis revealed no statistical between-gender differences. It is important to note that the pads can be used in practically all clinical setups, since their effect does not depend on the used hard- or software. Therefore, dielectric pads represent a convenient and economic approach to enable TMJ imaging at 7.0 T.[15]

Importantly, several other methods have been suggested to improve local B1+ fields,[27-30] including static B1+ shimming and the application of dedicated RF pulse designs, such as adiabatic pulses and spatially tailored excitation designs.[31,32] However, several issues, including the management of the specific absorption rate (SAR) levels, are still challenging and need to be solved to ensure a safe application in clinical routine.[15, 33, 34] Nevertheless, these approaches yield great potential for improving the image quality at 7.0 T and might make a significant contribution towards a further optimization of 7.0 T TMJ imaging in the future. [33-35]

*Quantitative analysis*

In the current study, we applied an intricate voxel-wise approach to determine SNR for different field strengths in vivo. In contrast to other methods to assess SNR, such as calculating the ratio between the mean signal intensity and the corresponding standard deviation within a specific region-of-interest or the subtraction method, the current approach, which is based on a second scan without radiofrequency pulses and gradient switching, accounts for potential noise correlation among all coil channels and yields therefore robust voxel-wise maps of the entire field of view.[13, 36, 37] Our SNR analysis yielded similar SNR for both field strengths within the TMJ. SNR was slightly lower for 7.0 T compared to 3.0 T, however, this comparison yielded no statistically significant difference. In general, utilizing a higher magnetic field strength increases longitudinal magnetization, resulting in higher SNR due to an increased number of protons aligning along the main axis of the static magnetic field.[13] However, the SNR depends also on many other variables, including the spatial resolution and sequence-specific parameters, such as TE and TR. Specifically, the SNR is positively correlated with the voxel-size and the TR and negatively correlated with the TE. In our study, the SNR was compared at a higher

spatial resolution for 7.0 T compared to 3.0 T using different sequence parameters (i.e. higher TR and lower TE for 7.0 T, see Table 1). According to theoretical considerations and given all sequence parameters for both field strengths (particularly the higher spatial resolution), SNR for 7.0 T is expected to be slightly lower compared to 3.0 T. Indeed, this trend was demonstrated in the SNR analysis, although statistical differences were not significant. Several additional aspects might have contributed to this observation: First, high-permittivity dielectric pads have been applied at 7.0 T only to mitigate the inhomogeneous flip-angle distribution in the area surrounding the temporomandibular joint. Although an SNR gain has been demonstrated,[20] residual under- and overtipping effects regarding the flip angle distribution might still slightly diminish the actual SNR. Second, the 32-channel head coil used at the 3.0 T system was based on the recently developed dStream system (Philips Healthcare, Best, The Netherlands), which digitalizes the acquired signal directly in the receive coil and transports it across broadband fiber optic cables, thus avoiding signal losses and noise pickups, which most likely improved the SNR at 3.0 T. This technique is still not available at 7.0T.

Previously, it has been demonstrated that musculoskeletal tissues yield different relaxation times at 7.0 T and 3.0 T.[19] Therefore, the TE and TR of newly designed sequences have to be chosen according to the T1 and T2 of different tissue types to evaluate the potential of clinical sequences at different field strengths.[13] In the current study, all parameters have been selected in such way that the whole SNR increase due to higher static magnetic field strength has been invested in higher spatial resolution while keeping the water-fat shift similar, which was considered most beneficial for MR imaging of the TMJ. It is to note that this approach resulted at in a longer TR at 7.0 T (3300 ms) compared to 3.0 T (2700 ms), which explained the longer acquisition time at 7.0 T. Although this optimization ensured a good image quality, it is important to take into

consideration that longer scan protocols bear the risk of increased patient movement. Naturally, the aforementioned gain in SNR could have been invested in increasing other parameters, which might be favorable when evaluating other anatomical regions of the dentomaxillofacial region.[38] In particular, decreasing the spatial resolution (i.e. decreasing the matrix size while keeping the FoV constant) and / or increasing the number of signal averages (i.e. number of excitations) represent easy applicable methods to strongly increase SNR in regions where the spatial resolution obtained at 3.0T is sufficient and / or which are not susceptible to movement artifacts. Finally, specific manufactured coils yield great potential in increasing SNR. Recently, Graessl and colleagues evaluated the performance of an individually constructed ophtalmic transmit/receive surface coil for MR imaging of the eye at 7.0 Tesla and demonstrated that the application of coils may greatly improve MR imaging of delicate structures, such as the eye[39]. Considering this observations, it can be assumed that MR imaging of the TMJ at 7.0 T might also greatly benefit from specifically tailored surface coils.

Taken together, considering all factors potentially modulating the SNR as well as their possible interactions is very challenging and was beyond the scope of the current study. Nevertheless, results suggest that the application of dielectric pads at 7.0 T enabled a robust and similar SNR when compared to 3.0 T while allowing for imaging the TMJ, particularly the temporomandibular disc, at a higher spatial resolution.

*Qualitative analysis*

The visual assessment of the TMJ yielded “substantial” to “almost perfect” inter-reader agreement for the evaluated structures at 7.0 T and 3.0 T. However, while at 3.0 T six out of eight evaluated structures yielded an “almost perfect” inter-reader agreement, at 7.0 T only the overall image quality showed an “almost perfect” inter-reader agreement, while

the inter-reader agreement for all 7 subregions of the TMJ was only "substantial". This observation might be explained by the extensive experience of TMJ imaging at our hospital, while the personal experience of the two radiologists with the visual assessment of the TMJ at 7.0 T is still small and may require further routine.

In the current study, imaging the TMJ at 7.0 T yielded statistically increased visibility of the anterior band, the intermediate zone and the posterior band of the temporomandibular disc. It is to note that the visibility of the larger anatomical structures, such as the mandibular condyle, the mandibular fossa and the inferior pterygoid muscle did not benefit from imaging at 7.0 T. These results are well in line with the assumption that fine anatomical structures cannot be depicted in full detail at 3.0 T,[7, 12, 19] while larger structures do not necessarily benefit from a higher spatial resolution. This observation also might explain why the overall image quality was rated similar for both field strengths. Nevertheless, presented results strongly suggest that imaging the TMJ at 7.0 T is superior to 3.0 T, especially when small anatomical structures are of particular interest.

*Methodological considerations and limitations*

We acknowledge several limitations of the current study as well as particular methodological considerations, which have to be taken into account when interpreting presented data. (i) *Dielectric pads.* The current study did not assess the impact of the dielectric pads on B1+ inhomogeneity. However, the applied procedure followed strictly a recently published feasibility study comparing images acquired with and without dielectric pads at 7.0 T and assessing the B1+ characteristics in the presence of the dielectric pads in full detail. [20] Therefore, no direct comparisons regarding images acquired with and without pads are presented in the current manuscript. Furthermore, imaging of the TMJ at 3.0 T was performed without pads, further complicating the interpretation of reported findings.

However, the dielectric pads used in the current study have been designed based on simulations for B1+ distribution at 7.0 T, therefore theoretical considerations suggest that their application at 3.0 T would not considerably improve image quality. Furthermore, the design of dedicated dielectric pads for 3.0 T was beyond the scope of the study, since B1+ dropouts in the region of the TMJ at 3.0 T are uncommon and dielectric pads with different permittivity properties would have further complicated the direct comparison between measured data at both field strengths. (ii) *Coils.* Currently, imaging of the TMJ is commonly performed using dedicated TMJ surface coils, while in this study only head coils were used. However, it has been demonstrated recently that MR imaging of the TMJ at 3.0T using a 32-channel head coil yields superior visibility of the anatomical structures of interest as well as higher SNR compared to broadly available 2-channel surface coil. [22] Still, it is to note that the headcoils used in this study were not identical. While the head coil at 3.0 T was a receive-only coil, the headcoil used at 7.0T was a transmit/receive coil with a different local distribution of receive elements. Therefore, observed differences in image quality might at least be partially explained by different hardware specifications. *(iii) Scan sequences.* In the current study, only proton-density weighted images have been acquired. The main focus of the current study was to evaluate the potential advantage of imaging structures at 7.0 T, which might benefit most from imaging at a high spatial resolution, such as the temporomandibular disc. Indeed, the temporomandibular disc yielded significantly improved image quality at 7.0 T compared to 3.0 T, while other structures such as the mandibular condyle, which can already be well depicted at 3.0 T, did not profit from increased spatial resolution. Nevertheless, additional sequences would provide additional insights regarding the clinical potential of TMJ imaging at 7.0 T and should be investigated in further studies. Furthermore, the application of 3D-acquisitions might yield a great potential in a clinical context, particularly since the orientation of the

correct axis can be very intricate. In the present study, however, we ensured a correct orientation by assuring a careful orientation of the acquired planes perpendicular to the transverse axis of the mandibular condyles according to recently reported studies.[21, 22] (iv) *SNR analysis.* When assessing a new sequence with respect to a potential clinical application at a new field strength, it is inherently necessary to optimize the imaging protocol with respect to the different relaxation times of musculoskeletal tissue at different static magnetic field strengths.[19] In the current study, selected sequence parameters, such as TE, TR have been chosen to fit different T1 and T2 values of specific tissues. However, it is to note that the temporomandibular joint consists of various tissue types with a heterogeneous difference between relaxation times at two different field strengths. Although results suggest that the chosen TR and TE might represent a good approximation, further standardized studies in phantoms and in-vivo are necessary to fully understand the impact of different scan parameters on the assessed SNR. (v) *Scan planning.* In clinical examinations, MR-images of the TMJ are often assessed in closed- and open-mouth position to evaluate potential alterations of the jaw-motion. In line with the literature,[20, 22] we considered the evaluation of images in closed-mouth position sufficient to infer possible benefits regarding the image quality achieved using dielectric pads. However, the potential use of dielectric pads regarding dynamic scan sequences is still unclear and should be investigated in a further study. (vi) *Study sample.* It is to note that since this is the first study comparing MR imaging of the TMJ at 7.0 T using dielectric pads and 3.0 T, the anticipated effect size could not be inferred from current literature. Therefore, no power analysis was performed to estimate the required number of participants. However, data were consistent with low standard deviations. Thus, our quantitative and qualitative data may serve as basis for statistical power analysis for future larger clinical trials. Furthermore, the current study assessed asymptomatic healthy volunteers only. Although

results demonstrate superior performance of MR imaging the TMJ at 7.0 T compared to 3.0 T, further studies assessing patients with TMDs are necessary to fully appraise the potential clinical benefit of imaging the TMJ at 7.0 T. Please note that the IRB approval did not allowed inclusion of patients. Thus, only asymptomatic volunteers could be included.

*Clinical implications*

Current MR imaging studies still provide only an unsatisfactory correlation between imaging findings and reported symptoms in patients with TMDs, [7] which is assumed to be explained by the insufficient spatial resolution, which can be achieved at 1.5 T or 3.0 T. In the current study, the application of a higher static magnetic field strength (i.e. 7.0 T) in combination with high-permittivity dielectric pads enabled an increased spatial resolution, finally yielding a superior visibility of temporomandibular disc in asymptomatic volunteers compared to 3.0 T. Current results strongly suggest that the achieved improvement in visibility of the temporomandibular disc might likely translate into a considerably improved diagnostic accuracy when evaluating potential pathologies underlying TMDs and have an impact on clinical decision making and therapeutic outcome for patients where MR imaging of the TMJ at 1.5 T or 3.0 T is not sufficient to reveal the specific pathology causing clinical complaints. However, future studies including patients with various TMD-related pathologies are needed to provide clear evidence for the clinical practicability of the application of dielectric pads and/or the superior performance of imaging the TMJ at 7.0 T in a clinical context.

## Conclusions

Magnetic resonance imaging of the TMJ at 7.0 T using high-permittivity dielectric pads at a higher spatial resolution yields similar SNR and increased visibility of small anatomical structures of the temporomandibular disc compared to 3.0 T.

## References


1. Ahmad M, Hollender L, Anderson Q, Kartha K, Ohrbach R, Truelove EL, et al. Research diagnostic criteria for temporomandibular disorders (RDC/TMD): development of image analysis criteria and examiner reliability for image analysis. *Oral Surg Oral Med Oral Pathol Oral Radiol Endod* 2009; **107**: 844–860.
2. McNeill C. Management of temporomandibular disorders: concepts and controversies. *J Prosthet Dent* 1997; **77**: 510–522.
3. Aiken A, Bouloux G, Hudgins P. MR imaging of the temporomandibular joint. *Magn Reson Imaging Clin N Am* 2012; **20**: 397–412.
4. de Farias JF, Melo SL, Bento PM, Oliveira LS, Campos PS, de Melo DP. Correlation between temporomandibular joint morphology and disc displacement by MRI. *Dentomaxillofac Radiol* 2015; **44**: 20150023.
5. Stehling C, Vieth V, Bachmann R, Nassenstein I, Kugel H, Kooijman H, et al. High-resolution magnetic resonance imaging of the temporomandibular joint: image quality at 1.5 and 3.0 Tesla in volunteers. *Invest Radiol* 2007; **42**: 428–434.
6. Schmid-Schwap M, Drahanowsky W, Bristela M, Kundi M, Piehslinger E, Robinson S. Diagnosis of temporomandibular dysfunction syndrome--image quality at 1.5 and 3.0 Tesla magnetic resonance imaging. *Eur Radiol* 2009; **19**: 1239–1245.
7. Koh KJ, List T, Petersson A, Rohlin M. Relationship between clinical and magnetic resonance imaging diagnoses and findings in degenerative and inflammatory temporomandibular joint diseases: a systematic literature review. *J Orofac Pain* 2009; **23**: 123–139.
8. Ramnath RR. 3T MR imaging of the musculoskeletal system (Part I): considerations, coils, and challenges. *Magn Reson Imaging Clin N Am* 2006; **14**: 27–40.
9. Nordmeyer-Massner JA, De Zanche N, Pruessmann KP. Mechanically adjustable coil array for wrist MRI. *Magn Reson Med* 2009; **61**: 429–438.
10. Regatte RR, Schweitzer ME. Ultra-high-field MRI of the musculoskeletal system at 7.0T. *J Magn Reson Imaging* 2007; **25**: 262–269.
11. Kraff O, Fischer A, Nagel AM, Monninghoff C, Ladd ME. MRI at 7 Tesla and above: demonstrated and potential capabilities. *J Magn Reson Imaging* 2015; **41**: 13–33.

12. Krug R, Stehling C, Kelley DA, Majumdar S, Link TM. Imaging of the musculoskeletal system in vivo using ultra-high field magnetic resonance at 7 T. *Invest Radiol* 2009; **44**: 613–618.
13. Nordmeyer-Massner JA, Wyss M, Andreisek G, Pruessmann KP, Hodler J. In vitro and in vivo comparison of wrist MR imaging at 3.0 and 7.0 tesla using a gradient echo sequence and identical eight-channel coil array designs. *J Magn Reson Imaging* 2011; **33**: 661–667.
14. Springer E, Bohndorf K, Juras V, Szomolanyi P, Zbyn S, Schreiner MM, et al. Comparison of Routine Knee Magnetic Resonance Imaging at 3 T and 7 T. *Invest Radiol* 2016;
15. Brink WM, van der Jagt AM, Versluis MJ, Verbist BM, Webb AG. High permittivity dielectric pads improve high spatial resolution magnetic resonance imaging of the inner ear at 7 T. *Invest Radiol* 2014; **49**: 271–277.
16. Welsch GH, Juras V, Szomolanyi P, Mamisch TC, Baer P, Kronnerwetter C, et al. Magnetic resonance imaging of the knee at 3 and 7 tesla: a comparison using dedicated multi-channel coils and optimised 2D and 3D protocols. *Eur Radiol* 2012; **22**: 1852–1859.
17. Teeuwisse WM, Brink WM, Webb AG. Quantitative assessment of the effects of high-permittivity pads in 7 Tesla MRI of the brain. *Magn Reson Med* 2012; **67**: 1285–1293.
18. Hsu YC, Chern IL, Zhao W, Gagoski B, Witzel T, Lin FH. Mitigate B1+ inhomogeneity using spatially selective radiofrequency excitation with generalized spatial encoding magnetic fields. *Magn Reson Med* 2014; **71**: 1458–1469.
19. Jordan CD, Saranathan M, Bangerter NK, Hargreaves BA, Gold GE. Musculoskeletal MRI at 3.0 T and 7.0 T: a comparison of relaxation times and image contrast. *Eur J Radiol* 2013; **82**: 734–739.
20. Manoliu A, Spinner G, Wyss M, Ettlin DA, Nanz D, Kuhn FP, et al. Magnetic Resonance Imaging of the Temporomandibular Joint at 7.0 T Using High-Permittivity Dielectric Pads: A Feasibility Study. *Invest Radiol* 2015;
21. Manoliu A, Spinner G, Wyss M, Erni S, Ettlin DA, Nanz D, et al. Quantitative and qualitative comparison of MR imaging of the temporomandibular joint at 1.5 Tesla and 3.0 Tesla using an optimized high-resolution protocol. *Dentomaxillofac Radiol* 2015; 20150240.

22. Manoliu A, Spinner G, Wyss M, Filli L, Erni S, Ettlin DA, et al. Comparison of a 32-channel head coil and a 2-channel surface coil for MR imaging of the temporomandibular joint at 3.0 Tesla. *Dentomaxillofac Radiol* 2016; 20150420.
23. Roemer PB, Edelstein WA, Hayes CE, Souza SP, Mueller OM. The NMR phased array. *Magn Reson Med* 1990; **16**: 192–225.
24. Pruessmann KP, Weiger M, Scheidegger MB, Boesiger P. SENSE: sensitivity encoding for fast MRI. *Magn Reson Med* 1999; **42**: 952–962.
25. Landis JR, Koch GG. The measurement of observer agreement for categorical data. *Biometrics* 1977; **33**: 159–174.
26. Snaar JE, Teeuwisse WM, Versluis MJ, van Buchem MA, Kan HE, Smith NB, et al. Improvements in high-field localized MRS of the medial temporal lobe in humans using new deformable high-dielectric materials. *NMR Biomed* 2011; **24**: 873–879.
27. Metzger GJ, Snyder C, Akgun C, Vaughan T, Ugurbil K, Van de Moortele PF. Local B1+ shimming for prostate imaging with transceiver arrays at 7T based on subject-dependent transmit phase measurements. *Magn Reson Med* 2008; **59**: 396–409.
28. De Martino F, Schmitter S, Moerel M, Tian J, Ugurbil K, Formisano E, et al. Spin echo functional MRI in bilateral auditory cortices at 7 T: an application of B(1) shimming. *Neuroimage* 2012; **63**: 1313–1320.
29. Ellermann J, Goerke U, Morgan P, Ugurbil K, Tian J, Schmitter S, et al. Simultaneous bilateral hip joint imaging at 7 Tesla using fast transmit B(1) shimming methods and multichannel transmission - a feasibility study. *NMR Biomed* 2012; **25**: 1202–1208.
30. Metzger GJ, Auerbach EJ, Akgun C, Simonson J, Bi X, Ugurbil K, et al. Dynamically applied B1+ shimming solutions for non-contrast enhanced renal angiography at 7.0 Tesla. *Magn Reson Med* 2013; **69**: 114–126.
31. Garwood M, DelaBarre L. The return of the frequency sweep: designing adiabatic pulses for contemporary NMR. *J Magn Reson* 2001; **153**: 155–177.
32. Saekho S, Boada FE, Noll DC, Stenger VA. Small tip angle three-dimensional tailored radiofrequency slab-select pulse for reduced B1 inhomogeneity at 3 T. *Magn Reson Med* 2005; **53**: 479–484.
33. Grissom WA, Khalighi MM, Sacolick LI, Rutt BK, Vogel MW. Small-tip-angle spokes pulse design using interleaved greedy and local optimization methods. *Magn Reson Med* 2012; **68**: 1553–1562.

34. Setsompop K, Wald LL, Alagappan V, Gagoski BA, Adalsteinsson E. Magnitude least squares optimization for parallel radio frequency excitation design demonstrated at 7 Tesla with eight channels. *Magn Reson Med* 2008; **59**: 908–915.
35. Setsompop K, Alagappan V, Gagoski B, Witzel T, Polimeni J, Potthast A, et al. Slice-selective RF pulses for in vivo B1+ inhomogeneity mitigation at 7 tesla using parallel RF excitation with a 16-element coil. *Magn Reson Med* 2008; **60**: 1422–1432.
36. Filli L, Piccirelli M, Kenkel D, Boss A, Manoliu A, Andreisek G, et al. Accelerated magnetic resonance diffusion tensor imaging of the median nerve using simultaneous multi-slice echo planar imaging with blipped CAIPIRINHA. *Eur Radiol* 2015;
37. Manoliu A, Ho M, Nanz D, Piccirelli M, Dappa E, Klarhofer M, et al. Diffusion Tensor Imaging of Lumbar Nerve Roots: Comparison Between Fast Readout-Segmented and Selective-Excitation Acquisitions. *Invest Radiol* 2016; **51**: 499–504.
38. Manoliu A, Ho M, Nanz D, Dappa E, Boss A, Grodzki DM, et al. MR neurographic orthopantomogram: Ultrashort echo-time imaging of mandibular bone and teeth complemented with high-resolution morphological and functional MR neurography. *J Magn Reson Imaging* 2016;
39. Graessl A, Muhle M, Schwerter M, Rieger J, Oezerdem C, Santoro D, et al. Ophthalmic magnetic resonance imaging at 7 T using a 6-channel transceiver radiofrequency coil array in healthy subjects and patients with intraocular masses. *Invest Radiol* 2014; **49**: 260–270.

## Tables

**Table 1** Scan parameters of the PDw-sequences in pseudo-sagittal orientation at 7.0 T and 3.0 T, respectively. The scan parameters are reported, for each field strength. Abbreviations: FoV, Field of View; TR, repetition time; TE, echo time; wfs, water-fat-shift; TSE, turbo-spin-echo; NSA, number of signal averages, ETL: echo train length.

| Parameter | PDw-TSE sagittal | |
|---|---|---|
| | **7.0 T** | **3.0 T** |
| FoV [mm] | 150 x 150 | 150 x 150 |
| Pixel Size [mm] | 0.4 x 0.4 | 0.5 x 0.5 |
| Reconstructed pixel size [mm] | 0.2 x 0.2 | 0.25 x 0.25 |
| Slice thickness [mm] | 2 | 2 |
| Number of slices | 2 x 12 | 2 x 12 |
| TR | 3300 | 2700 |
| TE | 22 | 26 |
| wfs in pixel [mm] | 1.52 | 1.199 |
| effective wfs in image [mm] | 0.6 | 0.6 |
| wfs in Hz | 674 | 362 |
| TSE factor / echo train length [ETL] | 7 | 7 |
| echo spacing [ES] | 12 | 7,4 |
| number of signal averages [NSA / ]number of excitations [NEX] | 1 | 1 |
| Scan time [min] | 05:49 | 03:52 |

**Table 2** Visibility of different anatomical structures of the temporomandibular joint at 7.0 T and 3.0 T and corresponding between-group differences, for both readers. Mean and standard deviation are given for the visibility of each anatomical structure on a 5-point Likert-scale ranging from 1 (excellent visibility and delineation) to 5 (complete lack of visibility) for both readers. For evaluation of corresponding between-group differences, p-values are given uncorrected as well as corrected for multiple comparisons. Asterisks indicate statistical significance after correction for multiple comparisons.

| Anatomic structure | 7.0T | | 3.0T | | 7.0T vs. 3.0T | |
|---|---|---|---|---|---|---|
| | Mean | SD | Mean | SD | p-value (un-corrected) | p-value (corrected) |
| Reader 1 | | | | | | |
| Temporomandibular disc | | | | | | |
| Anterior band | 1,29 | 0,46 | 2,17 | 0,38 | 0,000 | 0,001* |
| Intermediate zone | 1,46 | 0,51 | 2,21 | 0,42 | 0,000 | 0,001* |
| Posterior band | 1,58 | 0,58 | 2,46 | 0,59 | 0,000 | 0,002* |
| Bilaminar zone | 1,83 | 0,48 | 2,04 | 0,46 | 0,132 | 1,000 |
| Mandibular fossa | 1,50 | 0,59 | 1,29 | 0,46 | 0,132 | 1,000 |
| Mandibular condyle | 1,54 | 0,72 | 1,29 | 0,46 | 0,175 | 1,000 |
| Inferior pterygoid muscle | 1,75 | 0,68 | 1,75 | 0,74 | 0,976 | 1,000 |
| Overall image quality | 1,54 | 0,59 | 1,96 | 0,81 | 0,070 | 0,559 |
| Reader 2 | | | | | | |
| Temporomandibular disc | | | | | | |
| Anterior band | 1,33 | 0,48 | 2,13 | 0,34 | 0,000 | 0,000* |
| Intermediate zone | 1,50 | 0,51 | 2,17 | 0,38 | 0,000 | 0,001* |
| Posterior band | 1,54 | 0,51 | 2,42 | 0,58 | 0,000 | 0,002* |
| Bilaminar zone | 1,71 | 0,46 | 2,13 | 0,45 | 0,008 | 0,060 |
| Mandibular fossa | 1,50 | 0,59 | 1,25 | 0,44 | 0,058 | 0,462 |
| Mandibular condyle | 1,50 | 0,51 | 1,29 | 0,46 | 0,166 | 1,000 |
| Inferior pterygoid muscle | 1,71 | 0,69 | 1,79 | 0,72 | 0,717 | 1,000 |
| Overall image quality | 1,46 | 0,51 | 1,88 | 0,74 | 0,053 | 0,425 |

**Table 3** Visibility of different anatomical structures of the temporomandibular joint at 7.0 T and 3.0 T for women and men and corresponding between-group differences. Mean and standard deviation are given for the visibility of each anatomical structure for both readers. Grading was based on a 5-point Likert-scale ranging from 1 (excellent visibility and delineation) to 5 (complete lack of visibility). For evaluation of corresponding between-group differences, p-values are given uncorrected as well as corrected for multiple comparisons.

| Anatomic structure | Women | | Men | | Women vs. Men | |
|---|---|---|---|---|---|---|
| | Mean | SD | Mean | SD | p-value (un-corrected) | p-value (corrected) |
| Reader 1 | | | | | | |
| 7.0 Tesla | | | | | | |
| Temporomandibular disc | | | | | | |
| Anterior band | 1,25 | 0,45 | 1,33 | 0,49 | 0,67 | 1,00 |
| Intermediate zone | 1,50 | 0,52 | 1,42 | 0,51 | 0,70 | 1,00 |
| Posterior band | 1,67 | 0,49 | 1,50 | 0,67 | 0,50 | 1,00 |
| Bilaminar zone | 1,75 | 0,62 | 1,92 | 0,29 | 0,41 | 1,00 |
| Mandibular fossa | 1,50 | 0,67 | 1,50 | 0,52 | 1,00 | 1,00 |
| Mandibular condyle | 1,42 | 0,67 | 1,67 | 0,78 | 0,41 | 1,00 |
| Inferior pterygoid muscle | 1,42 | 0,51 | 2,08 | 0,67 | 0,01 | 0,10 |
| Overall image quality | 1,33 | 0,49 | 1,75 | 0,62 | 0,08 | 0,66 |
| 3.0 Tesla | | | | | | |
| Temporomandibular disc | | | | | | |
| Anterior band | 2,33 | 0,49 | 2,00 | 0,00 | 0,03 | 0,23 |
| Intermediate zone | 2,33 | 0,49 | 2,08 | 0,29 | 0,14 | 1,00 |
| Posterior band | 2,58 | 0,67 | 2,33 | 0,49 | 0,31 | 1,00 |
| Bilaminar zone | 1,83 | 0,39 | 2,25 | 0,45 | 0,02 | 0,19 |
| Mandibular fossa | 1,17 | 0,39 | 1,42 | 0,51 | 0,19 | 1,00 |
| Mandibular condyle | 1,17 | 0,39 | 0,11 | | 0,19 | 1,00 |
| Inferior pterygoid muscle | 1,75 | 0,87 | 1,75 | 0,62 | 1,00 | 1,00 |
| Overall image quality | 1,83 | 0,94 | 2,08 | 0,67 | 0,46 | 1,00 |
| Reader 2 | | | | | | |
| 7.0 Tesla | | | | | | |
| Temporomandibular disc | | | | | | |
| Anterior band | 1,25 | 0,45 | 1,42 | 0,51 | 0,41 | 1,00 |
| Intermediate zone | 1,50 | 0,52 | 1,50 | 0,52 | 1,00 | 1,00 |
| Posterior band | 1,67 | 0,49 | 1,42 | 0,51 | 0,24 | 1,00 |
| Bilaminar zone | 1,50 | 0,52 | 1,92 | 0,29 | 0,02 | 0,19 |
| Mandibular fossa | 1,42 | 0,51 | 1,58 | 0,67 | 0,50 | 1,00 |
| Mandibular condyle | 1,42 | 0,51 | 1,58 | 0,51 | 0,44 | 1,00 |

| | | | | | | |
|---|---|---|---|---|---|---|
| Inferior pterygoid muscle | 1,42 | 0,51 | 2,00 | 0,74 | 0,04 | 0,28 |
| Overall image quality | 1,25 | 0,45 | 1,67 | 0,49 | 0,04 | 0,34 |
| 3.0 Tesla | | | | | | |
| Temporomandibular disc | | | | | | |
| Anterior band | 2,25 | 0,45 | 2,00 | 0,00 | 0,07 | 0,55 |
| Intermediate zone | 2,25 | 0,45 | 2,08 | 0,29 | 0,29 | 1,00 |
| Posterior band | 2,50 | 0,67 | 2,33 | 0,49 | 0,50 | 1,00 |
| Bilaminar zone | 2,00 | 0,43 | 2,25 | 0,45 | 0,18 | 1,00 |
| Mandibular fossa | 1,08 | 0,29 | 1,42 | 0,51 | 0,06 | 0,51 |
| Mandibular condyle | 1,17 | 0,39 | 1,42 | 0,51 | 0,19 | 1,00 |
| Inferior pterygoid muscle | 1,83 | 0,83 | 1,75 | 0,62 | 0,78 | 1,00 |
| Overall image quality | 1,67 | 0,78 | 2,08 | 0,67 | 0,17 | 1,00 |

## Figures

**Figure 1** High-permittivity dielectric pads. In this study, high-permittivity dielectric pads were used with properties extensively described in previous studies (see [15] for SAR- and B1+ simulations as well as [20] for detailed presentation of the particular application for imaging the TMJ). Panel (A) shows the set for female volunteers, panel (B) shows the set for male volunteers.

**Figure 2** SNR maps for images of the TMJ acquired at 7.0 T and 3.0 T. For SNR analysis, data were calculated on a voxel-wise basis for every coil channel using dedicated software routines, yielding voxel-based SNR maps Panel (A) shows the voxel-wise SNR map for a representative volunteer at 7.0 T, panel (B) shows the voxel-wise SNR map for the same volunteer at 3.0 T. SNR within the region of interest (temporomandibular disc, the temporomandibular fossa and the temporomandibular condyle) was similar for both field strengths. SNR-values are color-coded from 0 (red) to 40 (yellow).

**Figure 3** Qualitative analysis. PDw oblique sagittal images in closed mouth position at 7.0 T and 3.0 T. Panel (A) shows the sagittal image of a temporomandibular joint of an asymptomatic volunteer acquired at 7.0 T. Panel (B) shows the image of the same temporomandibular joint of the same asymptomatic volunteer acquired at 3.0 T. For all subregions of the temporomandibular joint, visibility was statistically significant higher at 7.0 T.

Figure 1



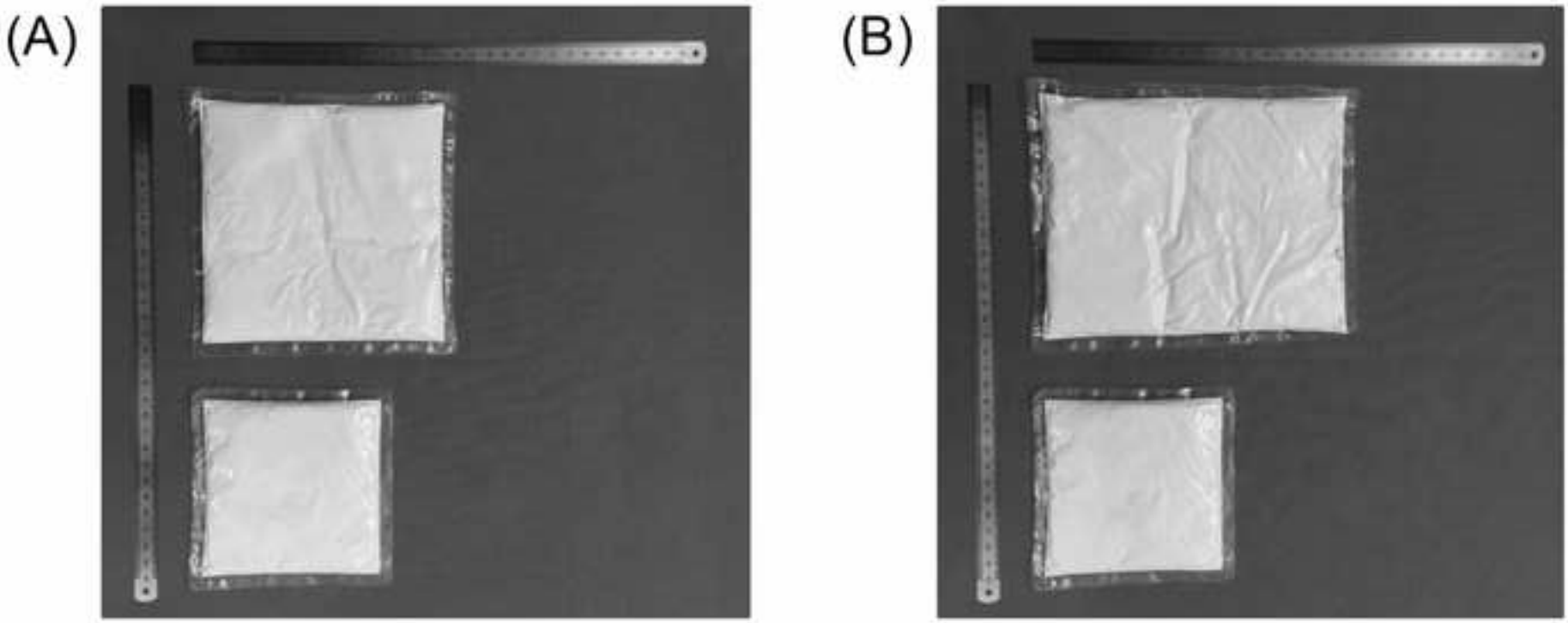

Figure 2



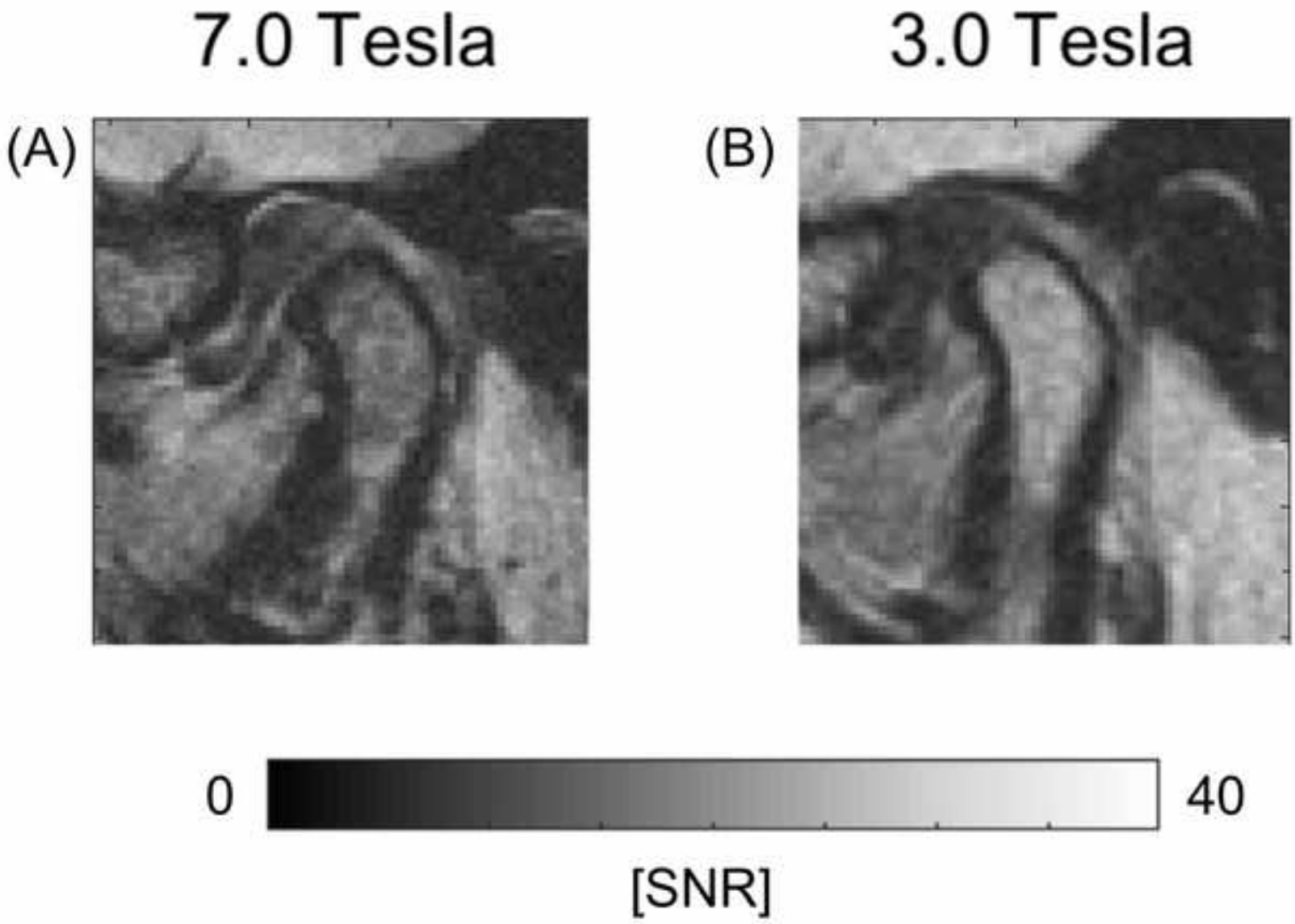

Figure 3